AD-A132 698 LOW-FREQUENCY RAMAN SCATTERING FROM VITREOUS AND MOLTEN 1//
B203(U) HOWARD UNIV WASHINGTON DC DEPT OF CHEMISTRY
G E WALRAFEN ET AL. 08 SEP 83 TR-15 N00014-80-C-0305

UNCLASSIFIED F/G 11/2 NL

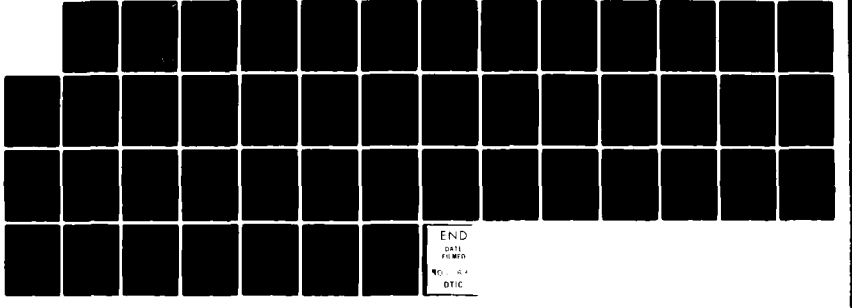

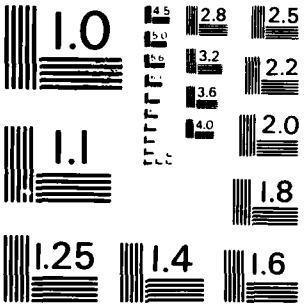

AD-A132 698

SECURITY CLASSIFICATION OF THIS PAGE (When Data Entered)

REPORT DOCUMENTATION PAGE

READ INSTRUCTIONS BEFORE COMPLETING FORM

1. REPORT NUMBER: 15	2. GOVT ACCESSION NO.: AD-A132 698
3. RECIPIENT'S CATALOG NUMBER:	
4. TITLE (and Subtitle): Low-Frequency Raman Scattering From Vitreous And Molten B_2O_3	5. TYPE OF REPORT & PERIOD COVERED: Technical Report #15
	6. PERFORMING ORG. REPORT NUMBER:
7. AUTHOR(s): G.E. Walrafen, M.S. Hokmabadi, P.N. Krishnan & S. Guha	8. CONTRACT OR GRANT NUMBER(s): N00014-80-C-0305
9. PERFORMING ORGANIZATION NAME AND ADDRESS: Department of Chemistry, Howard University, Washington, D.C. 20059	10. PROGRAM ELEMENT, PROJECT, TASK AREA & WORK UNIT NUMBERS: NR-051-733
11. CONTROLLING OFFICE NAME AND ADDRESS: Office of Naval Research, Department of the Navy, Arlington, Virginia 22217	12. REPORT DATE: September 8, 1983
	13. NUMBER OF PAGES: 22
14. MONITORING AGENCY NAME & ADDRESS (if different from Controlling Office)	15. SECURITY CLASS. (of this report): Unclassified
	15a. DECLASSIFICATION/DOWNGRADING SCHEDULE:

16. DISTRIBUTION STATEMENT (of this Report)

Approved for public release; reproduction is permitted for any purpose of the United States government distribution is unlimited.

17. DISTRIBUTION STATEMENT (of the abstract entered in Block 20, if different from Report)

Distribution of this document is unlimited

18. SUPPLEMENTARY NOTES

Prepared and accepted for publication in the Journal of Chemical Physics.

19. KEY WORDS (Continue on reverse side if necessary and identify by block number)

Raman Scattering, B_2O_3 Glass, Temperature Dependence, Low Frequency Peak

20. ABSTRACT (Continue on reverse side if necessary and identify by block number)

SEE REVERSE SIDE FOR ABSTRACT

DD FORM 1 JAN 73 1473 EDITION OF 1 NOV 65 IS OBSOLETE

S/N 0102-014-6601

SECURITY CLASSIFICATION OF THIS PAGE (When Data Entered)

ABSTRACT

Integrated Raman intensities of bands between ~0-900 cm^{-1} have been obtained for molten B_2O_3 from 288-906°C. Emphasis was placed on the highly depolarized low-frequency contour (adjoining the exciting line) which is intense, broad, skewed to high frequencies, and displays a weak, broad, shoulder centered between ~ 100-150 cm^{-1}. The total integrated contour intensity from 0-300 cm^{-1}, as well as the peak intensity, obey the one-phonon Bose-Einstein (B.-E.) relation within 6%. The integrated intensity of the polarized 800 cm^{-1} boroxol ring (B_3O_6) line, however, decreases with temperature rise, in quantitative agreement with previous work, J. Chem. Phys., 72, 113 (1980), and correction using neutron scattering results yields a $\Delta H°$ value of 5.0 kcal/mole ring rupture. The low-frequency contour probably involves nonsymmetric collective modes of very large assemblies, cages, or rings, as well as librations of B_3O_6 groups (~100-150 cm^{-1}), and the fact that the B.-E. distribution is obeyed at temperatures for which B_3O_6 ring rupture is important indicates that such large temporal aggregates are involved that whether BO_3 triangles or B_3O_6 rings are present may be nearly irrelevant. The peak frequency of the B.-E. corrected low-frequency contour was also observed to be constant, ~50 cm^{-1}, from 8°K to ~200°C, but it falls rapidly near $T_g \approx$ 280°C, and then reaches a ~27 cm^{-1} limit above 400°C. This suggests that the force constants of the low-frequency modes decrease upon melting because the anharmonicity increases due to the increased melt free volume produced by boroxol ring rupture. However, most features of the low-frequency Raman data, including depolarization, may also be explained in terms of ultrasonic acoustic modes and stress wave theory.

"LOW-FREQUENCY RAMAN SCATTERING FROM VITREOUS AND MOLTEN B_2O_3"

by

G.E. Walrafen, M.S. Hokmabadi, P.N. Krishnan, and S. Guha
Chemistry Department
Howard University
Washington, DC 20059

and

R.G. Munro
Center for Materials Science
National Bureau of Standards
Washington, DC 20234

Integrated Raman intensities of bands between ~0-900 cm^{-1} have been obtained for molten B_2O_3 from 288-906°C. Emphasis was placed on the highly depolarized low-frequency contour (adjoining the exciting line) which is intense, broad, skewed to high frequencies, and displays a weak, broad, shoulder centered between ~ 100-150 cm^{-1}. The total integrated contour intensity from 0-300 cm^{-1}, as well as the peak intensity, obey the one-phonon Bose-Einstein (B.-E.) relation within 6%. The integrated intensity of the polarized 800 cm^{-1} boroxol ring (B_3O_6) line, however, decreases with temperature rise, in quantitative agreement with previous work, J. Chem. Phys., 72, 113 (1980), and correction using neutron scattering results yields a $\Delta H°$ value of 5.0 kcal/mole ring rupture. The low-frequency contour probably involves nonsymmetric collective modes of very large assemblies, cages, or rings, as well as librations of B_3O_6 groups (~100-150 cm^{-1}), and the fact that the B.-E. distribution is obeyed at temperatures for which B_3O_6 ring rupture is important indicates that such large temporal aggregates are involved that whether BO_3 triangles or B_3O_6 rings are present may be nearly irrelevant. The peak frequency of the B.-E. corrected low-frequency contour was also observed to be constant, ~50 cm^{-1}, from 8°K to ~200°C, but it falls rapidly near $T_g \approx$ 280°C, and then reaches a ~27 cm^{-1} limit above 400°C. This suggests that the force constants of the low-frequency modes decrease upon melting because the anharmonicity increases due to the increased melt free volume produced by boroxol ring rupture. However, most features of the low-frequency Raman data, including depolarization, may also be explained in terms of ultrasonic acoustic modes and stress wave theory.

I. INTRODUCTION

Low-frequency Raman and infrared spectra from vitreous B_2O_3 were reported by Stolen[1] in 1970. He observed a depolarized Raman peak near 24 cm^{-1}, and an infrared peak near 26 cm^{-1}.[1] Shortly after, Shuker and Gammon[2] examined the temperature dependence of the low-frequency Raman region of B_2O_3 to about 1000°C. They concluded that first-order scattering from intermolecular vibrational states was involved.[2] Subsequently, Bril[3] examined the low-frequency Raman scattering from B_2O_3-Na_2O mixtures. He interpreted the low-frequency region in terms of translations or librations of part of the glass network, namely, 200 atoms or more.[3]

In Raman work at higher frequencies (primarily between 200 and 1600 cm^{-1}) Walrafen et al.[4] measured integrated intensity ratios from 77°K to ~ 1600°C. The intensity data were interpreted in terms of the rupture of boroxol (B_3O_6) rings, for which a $\Delta H°$ value of 6.4 ± 0.4 Kcal/mole boroxol resulted. This $\Delta H°$ was obtained by assuming that the uncorrected (no B.-E. correction) integrated intensity of the 300-800 cm^{-1} Raman contour was constant with temperature, and thus the 300-800 cm^{-1} contour area was used as an internal standard against which the area of the intense, sharp, polarized, 800 cm^{-1} B_3O_6 peak could be referenced. New Raman data in which integrated intensities, absolute in the sense that the laser beam intensity in the sample, and the effective collection geometry remain rigorously constant versus temperature, were required. Such data have now been obtained in this work between ~ 0-900 cm^{-1} at temperatures from 288 to 906°C. (These data provide quantitative support for the previously assumed constancy of the uncorrected 300-800 cm^{-1} area). However, the principal goal of the present work was to obtain a more complete understanding of the low-frequency (24 cm^{-1}) contour from vitreous and molten B_2O_3.

The nominal 24 cm^{-1} contour from vitreous B_2O_3 is remarkable in that it is unusually intense (roughly as intense as the sharp 800 cm^{-1} line at room temperature) but highly depolarized. It is also relatively sharp for a low-frequency glass mode, compared, for example, to the ~ 60 cm^{-1} mode from fused silica.(5) Thus, its understanding is of importance to the structure of vitreous B_2O_3, as well as to many other glass systems.

The new intensity data that have been obtained here suggest that the low-frequency Raman scattering involves (in major part) collective modes of large temporal or correlated assemblies of atoms whose basic units are BO_3 triangles and/or B_3O_6 rings. These correlated regions may refer to masses which range from 5400 to 23000 g-$mole^{-1}$; hence, as many as 100 -400 BO_3 masses may be involved. The new low-frequency Raman data and their interpretation are now presented.

II. EXPERIMENTAL

The sample preparation, heating method, and Raman procedure employed here were similar to those described previously in studies of molten B_2O_3.[4] However, because integrated Raman intensities under conditions of constant laser intensity and constant effective collection geometry were now required, a modified procedure was employed to obtain accurate integrated (absolute) intensities, in contrast to ratios of integrated intensities.[4]

The refractive index of molten B_2O_3 changes rapidly with temperature compared to that of fused silica.[6] Hence, methods in which the laser beam and/or the Raman scattering pass through both the molten B_2O_3 and the fused silica tube are not accurate.[2] (This conclusion was definitely confirmed by numerous trial runs in this work). Thus, a method was used which involved backscattering from the molten B_2O_3 -- air interface.

A convergent horizontal laser beam was reflected downward through a large hole in a 45-degree collection mirror, and brought to a sharp focus just below the molten B_2O_3 surface (the large hole prevented back-reflected plasma lines from being detected). The back-reflected laser beam was then adjusted such that it was precisely co-axial with the incident laser beam. This condition was rigorously maintained throughout the quantitative intensity measurements at all temperatures. The back-scattered Raman light was then reflected by the 45-degree collection mirror, and focused on the slit of the spectrometer. The width and shape of the enlarged image of the light pattern on the spectrometer slit jaws were carefully and continuously monitored throughout the measurements at all temperatures. No change or motion whatever of this light pattern was observed between 288 to 820°C, suggesting that the effective collection geometry remained invariant.

The molten B_2O_3 was contained in a vertical fused silica tube as

described previously.[4] A Pt-Rh thermocouple was placed near the laser beam spot, just below the molten B_2O_3 surface, for temperature measurement. The laser power was maintained constant to ± 3%, and measurements of the B.-E. corrected integrated intensity of the low-frequency contour over a 500°C range indicated constancy to within 6%.

Some Raman spectra of the vitreous material were also taken at temperatures as low as 8°K. The B_2O_3 sample and Raman method involved are described elsewhere.[7]

III. Results

Polarized and depolarized 90-degree, as well as polarized 0-degree, Stokes and anti-Stokes spectra were obtained in this work for Raman shifts, $\Delta\bar{\nu}$, between $\sim$ 0 and 900 cm^{-1}. Only the polarized 0-degree or back-scattering results yielded reliable absolute intensities, for reasons described in section II. Hence, only the back-scattering spectra are shown in Fig. 1.

In Fig. 1, three stokes Raman spectra, A to C, obtained between 7.5-350 cm^{-1} are shown. In these three cases, as well as in intermediate cases omitted for clarity, the amplitude of the <u>total</u> scattering, I_T, was first detectable at 7.5 cm^{-1} (see top left), and the shapes slightly above 7.5 cm^{-1} were identical. Hence, the spectra could be exactly superimposed at, and slightly above 7.5 cm^{-1}, and this procedure agreed with precise superposition beyond 200 cm^{-1}, as evident from the figure. From these superpositions, and from the shape of the C spectrum just above 7.5 cm^{-1} (4 intensity divisions from the bottom), a baseline was determined as shown by the dashed line, D. This same baseline was then employed for all of the back-scattering spectra, and from it the differences between the total scattering and baseline D were determined. The shape of baseline D was also determined in part by anti-Stokes spectra (not shown) which were obtained simultaneously with the Stokes spectra. Here it should be emphasized, that baseline D is not claimed to be precisely correct <u>per se</u>; instead, the differences between it and the total scattering at various temperatures are considered to represent the <u>changes</u> in the Raman intensity with temperature, reasonably accurately. Other procedures, such as multiplying the <u>total</u> scattering, I_T, by $\Delta\bar{\nu}/(1 + n)$, where n is the B.-E. factor, $(e^{hc\Delta\bar{\nu}/kT} - 1)^{-1}$, could be used, of course, but this method still requires non-linear baseline subtraction of the form $I_B\,\Delta\bar{\nu}/(1 + n)$, where I_B is the baseline intensity, which is roughly constant only above 200 cm^{-1}, as seen from Fig. 1.

The functional form of baseline D was found by least squares fitting procedures to be approximately exponential. Between 10 and 200 cm^{-1} baseline D is represented by the equation $I_B = A\, e^{-\Delta\bar{\nu}/\Delta\bar{\nu}_o}$, where $\Delta\bar{\nu}_o$ = 25 cm^{-1}. This form is consistent with (but does not imply the same mechanism as) the form used for depolarized scattering by Litovitz et al.[8] In this regard, it should be mentioned that the shape of the total polarized scattering, I_T, was nearly indistinguishable from that of the total depolar-

CAPTION

Fig. 1. Polarized low-frequency Raman spectra obtained by back-scattering from molten B_2O_3. The vertical arrow near 120 cm^{-1} refers to a weak shoulder thought to refer in part to boroxol ring librations. The slanting arrows near the inflections refer to the contour peak frequency at high temperatures. A slit-width corresponding to 5 cm^{-1} was employed with 514.5 nm excitation at a power level of 1W. The noise level of the spectra was about 4 times the line thickness at 25 cm^{-1}, and about equal to the line thickness at 150 cm^{-1}. The total scattering is quantitatively comparable between the spectra to about 4%.

Fig. 2

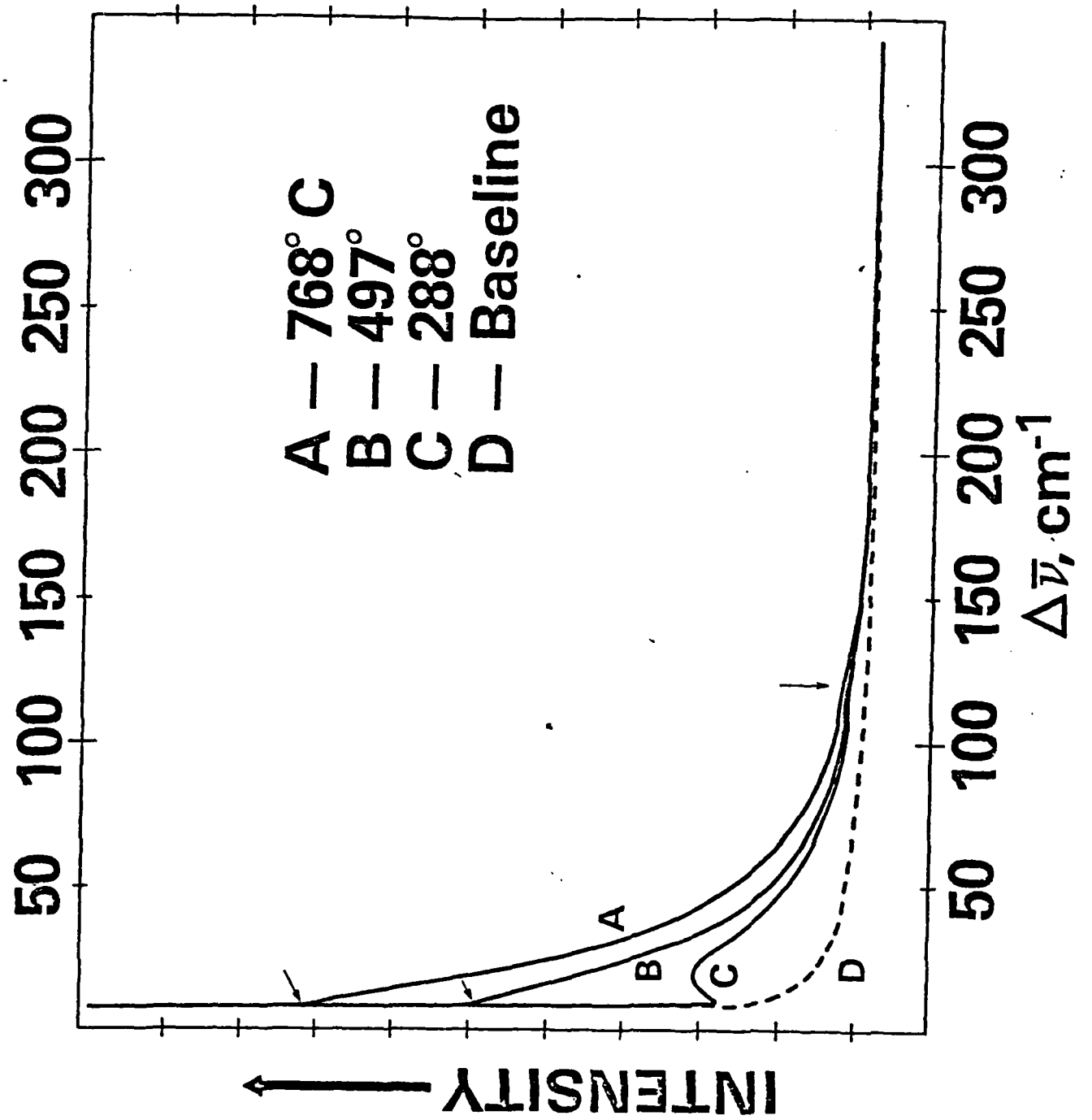
A — 768° C
B — 497°
C — 288°
D — Baseline
INTENSITY
50 100 150 200 250 300
50 100 150 200 250 300
Δν̄, cm⁻¹
A
B
C
D

ized scattering from 0-300 cm^{-1}, except for some suggestions that the shoulder region between $\sim$100-200 cm^{-1} was not quite totally depolarized. Further, the form of the baseline below the polarized spectra was indistinguishable from the baseline for the depolarized case.

From spectrum A, and from a spectrum intermediate between spectra B and C, spectra of the form $I_R/(1 + n)$ and $I_R \Delta\bar{\nu}/(1 + n)$, where $I_R = I_T - I_B$, are shown in Fig. 2(a) and 2(b), respectively. The (a) spectra of Fig. 2 involve only B.-E. correction, whereas the (b) spectra, which are the (a) spectra multiplied by $\Delta\bar{\nu}$, are sometimes referred to as reduced spectra. The Fig. 2 spectra are related to the vibrational density of states as formulated by Shuker and Gammon,[9] namely,

$$g(\omega) = \frac{I(\omega, T)\ \omega}{c(\omega)[1 + n(\omega,T)]} \quad . \quad (1)$$

Here, n is the B.-E. factor, $n = (e^{\hbar\omega/kT} - 1)^{-1}$, $I(\omega,T)$ is the experimentally determined depolarized Raman intensity for which $I_T - I_B$, is now substituted, $c(\omega)$ is the frequency dependent coupling coefficient, and $g(\omega)$ is the vibrational density of states. In this regard it should be noted that because the integrated Raman intensity is proportional to concentration at a given temperature, $\int^{\omega} g(\omega)d\omega$ has units of the number of oscillators per unit volume. Hence, if all of the intermolecular vibrations occur below 300 cm^{-1}, the integral of $g(\omega)$ from 0-300 cm^{-1} would encompass the total number of intermolecular oscillators per unit volume of vitreous or molten B_2O_3.

Both the (a) and (b) spectra of Fig. 2 invite division into two regions or components. The (a) spectra indicate a peak near 27 cm^{-1} and a shoulder centered between 100-150 cm^{-1}, and Gaussian deconvolution of the (b) spectra indicates two broad components centered near $\sim$56 cm^{-1} and $\sim$137 cm^{-1}, respectively. Unfortunately, the calculated spectra of Fig. 2 involve increasing amplification of errors with increasing frequency, as seen from the error limits shown. However, Gaussian computer analysis has indicated that the qualitative two-component nature of the coutours cannot be vitiated by such errors. Similarly, the raw spectra of Fig. 1 show a peak plus a weak shoulder, the latter indicated by a vertical arrow between 100-150 cm^{-1}.

Comparisons between Figs. 1 and 2(a) clearly indicate that the B.-E. correction increases the frequency of the peak intensity. For example, Fig. 1(a)

CAPTION

Fig. 2. Bose-Einstein corrected Raman spectra, $I_R/(1 + n)$, (a), and reduced Raman spectra, $I_R\Delta\bar{\nu}/(1 + n)$, (b), calculated from Fig. 1, where $I_R = I_T - I_B$.

Fig. 2

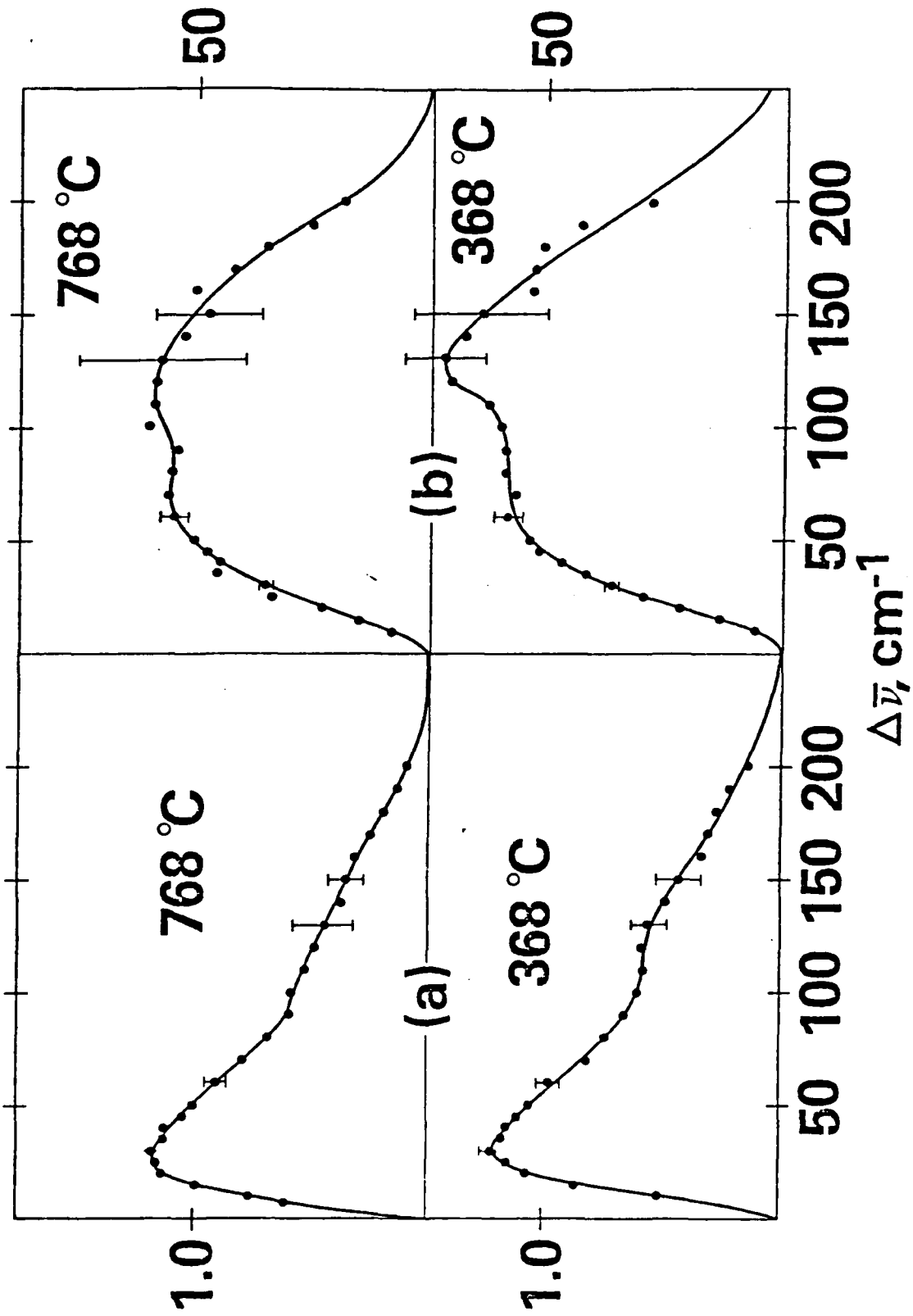
768 °C
368 °C
768 °C
368 °C
(a)
(b)
1.0
1.0
50 100 150 200
50 100 150 200
50
50
$\Delta\bar{\nu}$, cm^{-1}

indicates a peak (inflection shown by an arrow) near 8 cm^{-1} at 768°C, whereas Fig 2(a) indicates the corrected peak near 27 cm^{-1}. Such effects occur at temperatures where $kT >> \hbar c \Delta\bar{\nu}$. The function $I_R \Delta\bar{\nu}/(1 + n)$ also moves the peak position even farther upward. This is evident from a comparison between (b) and (a) of Fig. 2 below 100 cm^{-1}. However, such differences between the I_R and $I_R/(1 + n)$ spectra disappear as $T \rightarrow 0$, and thus where $(1 + n) \rightarrow 1$.

Peak positions for the I_R and $I_R/(1 + n)$ spectra are shown from -265°C (8°K) to about 1000°C in Fig. 3. In that figure the peak position of the uncorrected I_R spectrum approaches that of the $I_R/(1 + n)$ or the B.-E. corrected spectrum below -200°C. (Frequency data from the $I_R \Delta\bar{\nu}/(1 + n)$ spectra are not shown in Fig. 3.) The drop in $\Delta\bar{\nu}$ above T_G which occurs for the I_R peak frequency also occurs for the components of the $I_R/(1 + n)$ and perhaps weakly for the $I_R \Delta\bar{\nu}/(1 + n)$ spectra, but this is discussed in section IV.

One of the goals of the present work was to determine the way in which the total contour intensity or area between 300-800 cm^{-1}, $I_{300-800}$, varies with temperature (without B.-E. correction), in an effort to test the previous assumption of temperature invariance.[4] The quantity $I_{300-800}$ is shown along with the corresponding uncorrected integrated contour intensities, I_{27} (where 27 cm^{-1} is only the nominal peak value), and I_{800}, in Fig. 4(b). (Here, all of the data refer to backscattering, whose angular intensity dependence for polarized lines is not the same as for 90-degree scattering[10]). Within the scatter of the data, it is apparent that $I_{300-800}$ is invariant in the temperature range of 288° to 768°C. This result confirms the previous assumption to this effect,[4] and requires that the temperature dependence of I_{800} be the same as that of r_i, because $r_i = I_{800}/I_{300-800}$.[4] This agreement is clearly evident from Fig. 5, and is discussed in section IV.

From Fig. 4(b) it is also apparent that I_{27} increases rapidly with temperature rise whereas the B_3O_6 ring intensity, I_{800}, decreases. When I_{27}, the total Raman contour area of the low-frequency region, or $\int_0^{300} I_R d\bar{\nu}$, is corrected for the B.-E. factor, i.e., $I_R/(1 + n)$, temperature invariance within a mean deviation of 6% results, as evident from Fig. 4(a). Approximate invariance of the B.-E. corrected total intensity is not unexpected, however, because all of the intermolecular vibrations are thought

CAPTION

Fig. 3. Peak frequencies of uncorrected Raman spectra, lower dashed curve, and from Bose-Einstein corrected spectra, upper dashed curve, from 8°K or -265°C to about 1000°C. (*) refers to Ref. (2).

Fig. 3

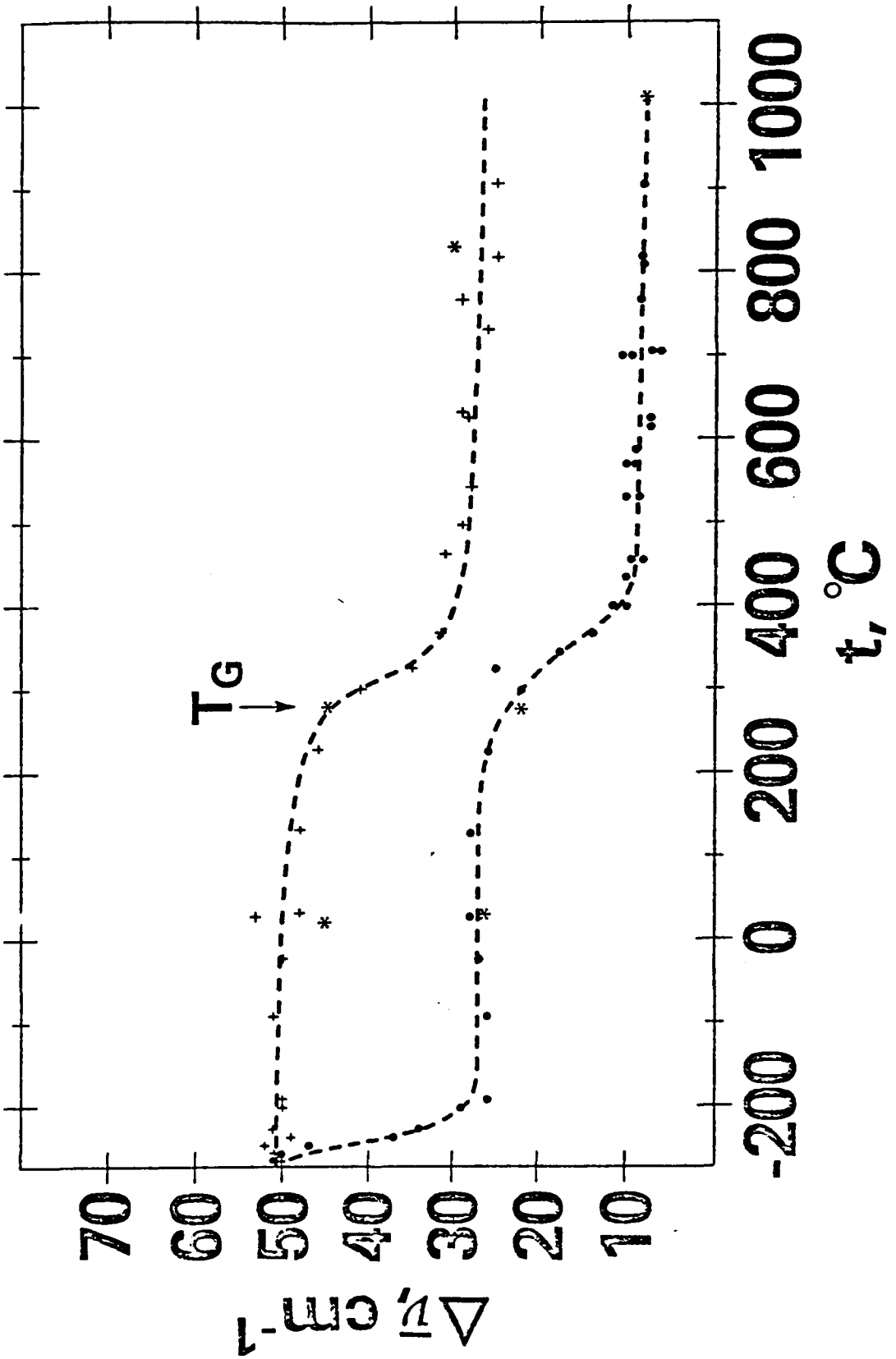

CAPTION

Fig. 4. Integrated intensities, (b) , for the total low-frequency contour ($\sim$0 - 300 cm^{-1}), I_{27}, for the 300 - 800 cm^{-1} contour, $I_{300-800}$, and for the peak at $\sim$800 cm^{-1}, I_{800}. The total low-frequency contour area corrected for the Bose-Einstein factor is shown in (a).

Fig.

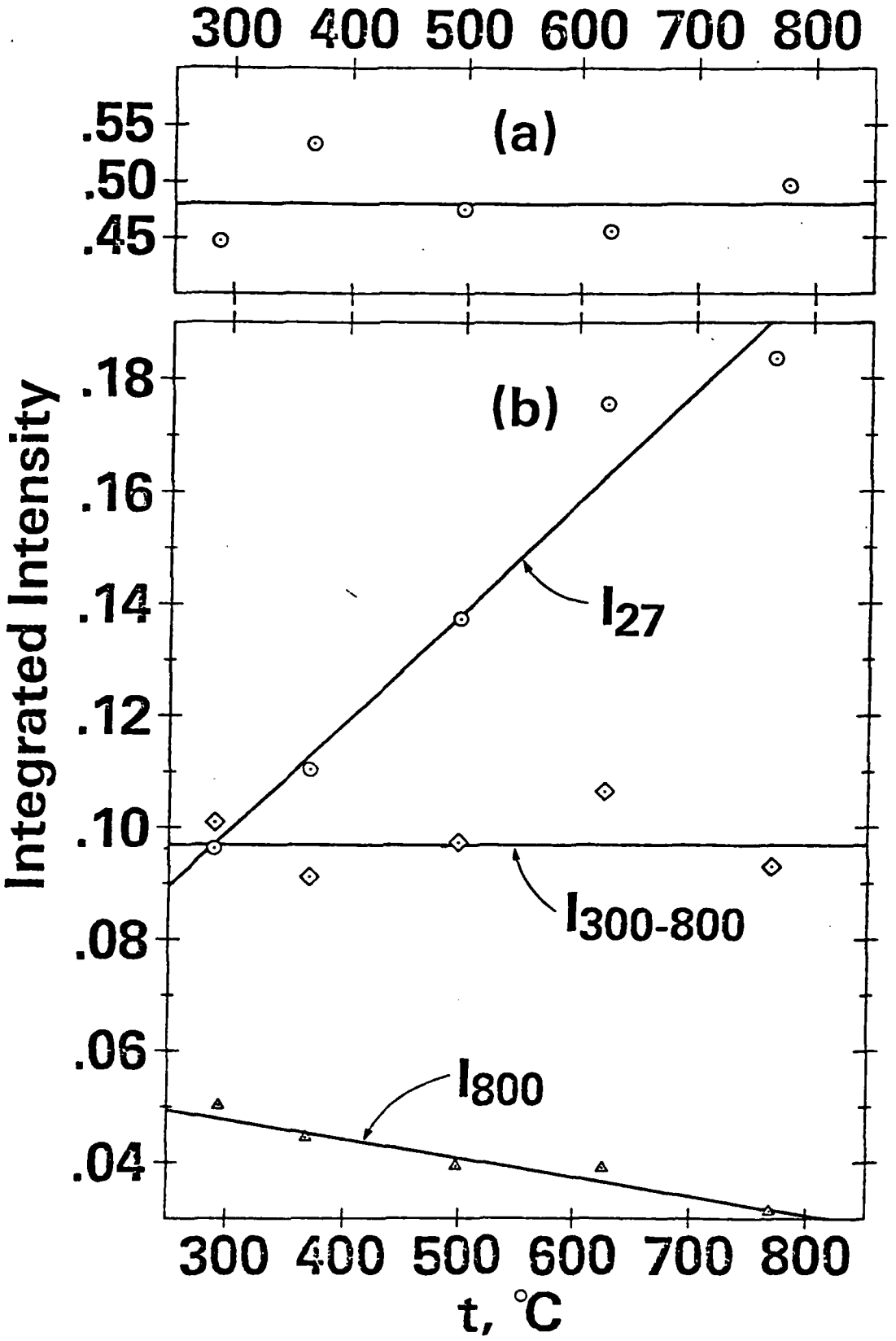
300 400 500 600 700 800
(a)
.55
.50
.45
(b)
.18
.16
.14
.12
.10
.08
.06
.04
Integrated Intensity
I_{27}
$I_{300-800}$
I_{800}
300 400 500 600 700 800
t, °C

to be included, i.e., the B_3O_6 and BO_3 librations, plus all of the collective intermolecular motions.

The integrated intensities of the total low-frequency contour were obtained for spectra of the type I_R/T, $I_R/(1 + n)$, and $I_R \Delta\bar{\nu}/(1 + n)$. The results are tabulated in Table I. These data are of possible value in determining which formulation of $c(\omega)$ in eqn. (1) leads to the correct form of $g(\omega)$, and are discussed in section IV.

IV. INTERPRETATION

A. Nature of the Intermolecular Motions.

Consider that a boroxol ring, B_3O_6, engages in libration or translation with respect to the surrounding glass or melt network. In such motions, three extra-annular B-O-B groups would be expected to bend. Bril[3] has reported a force constant for B-O-B bending of 3.3×10^4 dyne/cm. Assuming that the boroxol ring libration is harmonic (which, of course, is only an approximation), the librational frequency would be given by,

$$\Delta\bar{\nu} = \left(\frac{16.97\ NK}{M}\right)^{1/2} = \left(\frac{16.97K}{M'}\right)^{1/2} \qquad (2)$$

where N is the number of B-O-B units bent, i.e., 3 restoring forces, K is the bending force constant in dyne/cm, M is the "molecular weight" in gm-mole^{-1}, and $M' = M/N$. From eqn. (2) and Bril's bending force constant, a librational frequency of 114 cm^{-1} results for the complete B_3O_6 unit for which $M = 128.5$ gm-mole^{-1}, or of 145 cm^{-1} for the B_3C_3 ring within the B_3O_6 unit for which $M = 80.5$ gm-mole^{-1}. These values are in reasonable agreement with the range of 100-150 cm^{-1} for the center of the weak shoulder of Fig. 1, or for the corresponding features of Fig. 2. (Gaussian deconvolution of the Fig. 2(b) spectra, also yields a value of $\sim$ 137 cm^{-1}).

In previous work it was established that the concentration of boroxol rings decreases with increasing temperature of the melt.[4] Accordingly, the intensity of B_3O_6 libration should also decrease with temperature rise. Some evidence for this effect is seen from Figs. 1 and 2, where the feature centered between 100-150 cm^{-1} appears slightly more prominent at lower temperatures.

In regard to other librations, it should be noted that BO_3 triangles may possibly engage in librations as well. Again, three

Caption

Table I.

Total contour area between 0-300 cm^{-1} from spectra of the type indicated by I_{27}/T, etc., for temperatures from 288° to 768°C.

TABLE I

Table I

$t°C$	$\int_0^{300} \frac{I_R}{T} d\bar{\nu}$	$\int_0^{300} \frac{I_R}{(1+n)} d\bar{\nu}$	$\int_0^{300} \frac{I_R \Delta\bar{\nu}}{(1+n)} d\bar{\nu}$
288	1.72×10^{-4}	.45	.77
368	1.72×10^{-4}	.53	.83
497	1.78×10^{-4}	.48	.69
625	1.96×10^{-4}	.45	.80
768	1.77×10^{-4}	.50	.73
mean deviation	4%	6%	8%

connecting B-O-B units would be bent in such a libration. From eqn. (2), and the bending force constant, a librational frequency of 170 cm^{-1} results for M = 58.8. This value corresponds to the high-frequency tail of Figs. 1 and 2, and hence such a motion may not be very important.

Next, consider that a very large temporally correlated assembly of BO_3 triangles and/or B_3O_6 rings engages in a libration or translation such that bending of B-O-B linkages occurs only near its extremities. Such a motion of a large assembly seems a possible mode, but certainly not the only mode, of a large system of coupled anharmonic oscillators. Further, assume that no relative motion of BO_3 or B_3O_6 units occurs on the average within the confines of this large assembly. Also consider that the vibrational times between atoms in this assembly are at least one order of magnitude shorter than the oscillatory motion of the assembly as a whole. The ratio of the "molecular weight" of this temporal assembly, to the number of B-O-B linkages near its extremities that bend and produce a restoring force, is M'. Thus, from eqn. (2) and with K = 3.3×10^4 dyne/cm, M' would vary from about 768 to 179, depending upon which feature of Fig. 2(a) or 2(b), i.e., 27 cm^{-1} or 56 cm^{-1}, respectively, more nearly corresponds to the correct peak in the intermolecular vibrational density of states. However, N = 3 for either a BO_3 or B_3O_6 libration, and for a larger assembly it would certainly be much greater. If N is arbitrarily taken as 30, the "molecular weight" of the correlated region would range between 5400 and 23000 gm-$mole^{-1}$. Of course, such arguments are very qualitative, but it does not seem unreasonable to suppose that the main peak of the true vibrational density of states arises from a collective motion involving between 100-400 correlated BO_3 building-units, and whose dimensions or correlated diameter is of the order of 10-15 Å, for a nearly shperical shape and a B-O distance of 1.4 Å.[3] Here, it should be emphasized that this assembly may be associated with a definite structure; or, it may simply refer to a correlated motion of BO_3 units.

B. Vibrational Density of States.

In Table I three sets of results, referring to the I_R/T, $I_R/(1+n)$, and $I_R\,\Delta\bar{\nu}/(1+n)$ spectra, are presented for a range of temperatures. Each set shows invariance of the corresponding integrals with temperature, within the stated error limits. Consider first, the invariance associated with the I_R/T spectra, which appears to be the key to the explation of the other invariances.

At high temperatures, that is, temperatures for which $kT >> \hbar\omega$ or $hc\,\Delta\bar{\nu}$,

$$\lim_{T\to\infty} (1+n) = kT/\hbar\omega \qquad (3)$$

Hence, substitution of this result for $(1+n)$ in $I_R/(1+n)$ and in $I_R\,\Delta\bar{\nu}/(1+n)$ leads, respectively, to terms such as $I_R\,\Delta\bar{\nu}/T$ and $I_R(\Delta\bar{\nu})^2/T$. Further, if $\int_0^{300} \frac{I_R}{T}\, d\bar{\nu}$ is invariant with T, one would also expect corresponding invariance upon multiplication of I_R/T by $\Delta\bar{\nu}$ or $(\Delta\bar{\nu})^2$, unless, the structure of the I_R/T spectrum varies so much with T, particularly at high frequencies, that the large $\Delta\bar{\nu}$ or $(\Delta\bar{\nu})^2$ terms dominate. However, such dominance of large $\Delta\bar{\nu}$ or $(\Delta\bar{\nu})^2$ terms is clearly unlikely because the mean deviations listed for Table I increase about as would be expected for the errors involved, see the Fig. 2 error limits. Apparently, the observed constancy in the integral of I_R/T is the main factor which yields the corresponding constancies in the integrals of $I_R/(1+n)$ and $I_R\,\Delta\bar{\nu}/(1+n)$.

In terms of eqn. (3), and the ratio I_R/T, one can write $g(\omega)$ as,

$$g(\omega) \propto \frac{(I_R/T)\,\omega^2}{c(\omega)} \qquad (4)$$

In the region of $\sim$ 0-300 cm^{-1}, $\int_0^{300} I_R\, d\bar{\nu}$, refers to the integral over all of the intermolecular vibrations. The corresponding integral over the true density of intermolecular vibrational states would refer to all of the intermolecular oscillators per unit volume. Apart from the breakdown of B_3O_6 units to form BO_3 triangles, one would expect the number of intermolecular oscillators of other types to be about constant. Hence, first excluding the B_3O_6 and BO_3 librations, the remaining number of oscillators might be con-

stant, and thus the density of such states would decrease as the volume increases, e.g., by ~14% from ~300° to 800°C. Then, if the $B_3O_6 \rightarrow 3BO_3$ stoichiometry is also included, the number of intermolecular oscillators might increase with temperature rise, and if this increase just opposes the volume increase, $\int_0^{300} g(\omega)d\omega$ would be about constant.

If $\int_0^{300} g(\omega)d\omega$ is constant, and if the approximation of eqn. (3) is employed, the various functionalities of $c(\omega)$ that result are given in Table II. However, because the errors are amplified from I_R/T to $I_R/(1+n)$ to $I_R \Delta\bar{\nu}/(1+n)$, a choice yielding the correct functionality of $c(\omega)$, Table II, cannot be made simply by choosing the smallest mean deviation of Table I. This choice would favor the I_R/T spectra, i.e., $c(\omega) \propto \omega^2$, but other factors must be considered as well.

Values of $I_T - I_B$ from Fig. 1 were divided by T to yield spectra of the form $(I_T - I_B)/T$ or I_R/T. Of course, the I_R and I_R/T spectra have the same shape. Also the integral of I_R/T from 0-300 cm^{-1} is constant, Table I. However, the relative increase in the peak height apparent in Fig. 1 at the vertical arrow (120 cm^{-1}) nearly disappears when division by T is accomplished. The shapes of the I_R/T spectra (when multiplied by 10) were closely examined between ~80-150 cm^{-1}. The downward concavity (as seen from Fig. 1) was clearly much greater at low, then at high temperatures. However, the 10X spectra also indicate that there is a significant additional sloping background contribution beneath the component that produces the downward concavity. Accordingly, the high frequency density of states (near 120 cm^{-1}) appears to be degenerate, and the contribution of B_3O_6 librators may only be of the order of ~25% at 120 cm^{-1}. Finally, the spectra were divided into two areas, A, from 0-80 cm^{-1}, and B, from 80-300 cm^{-1}. The ratio of these areas, A/B, was found to decrease by ~16%, from 368 to 768°C. Hence, from the foregoing observations, it concluded that the I_R/T spectra are qualitatively consistent with a decrease in the number of B_3O_6 librators per unit volume with temperature rise, but that some other motion contributes more prominently in the high-frequency (120 cm^{-1}) region than the B_3O_6 libration.

Table II

Functionality of $C(\omega)$, the frequency dependent coupling coefficient, corresponding to various types of spectra, I_R/T, $I_R/(1 + n)$, or $I_R \Delta\bar{\nu}/(1 + n)$, see text.

TABLE I

Table II

Constant Term	Functionality of $C(\omega)$
$\int_0^{300} \frac{I_R d\bar{\nu}}{T}$	$C(\omega) \propto \omega^2$
$\int_0^{300} \frac{I_R d\bar{\nu}}{(1+n)}$	$C(\omega) \propto \omega$
$\int_0^{300} \frac{I_R \Delta\bar{\nu}\, d\bar{\nu}}{(1+n)}$	$C(\omega)$ = constant

Thus, the I_R/T data corresponding to $c(\omega) \propto \omega^2$ seem to have at least some of the qualitative attributes demanded of the true density of states.

Next, all spectra of this work of the form $I_R \Delta\bar{\nu}/(1 + n)$ were deconvoluted approximately by the use of two broad Gaussian components. These components were centered near ~56 and ~137 cm^{-1}. A similar decomposition was tried for the B.-E. or $I_R/(1 + n)$ spectra, but this failed, because the major component (peaking near 27 cm^{-1}) is strongly skewed to high frequencies. The ratio of the areas of the ~56 and ~137 cm^{-1} components was determined. This ratio did not vary significantly with temperature and was roughly 0.6 from 288° to 768°C. Hence, spectra of the form $I_R \Delta\bar{\nu}/(1 + n)$ do not seem to be very significant, and a constant value for $c(\omega)$ is thus not favored.

A dicision between the coupling coefficient functionalities, $c(\omega) \propto \omega^2$ or $c(\omega) \propto \omega$, is left to section IVD.

C. Concentration of Boroxol Rings

In previous Raman work, the ratio of integrated intensities, $I_{800}/I_{300-800}$, was determined and given the symbol r_i. It was then assumed that $I_{300-800}$, uncorrected for the B.-E. factor, was independent of temperature, and that it could act as an internal Raman standard. Next, because r_i was considered proportional to I_{800}, it was taken as a measure of the boroxol B_3O_6 ring concentration, and an equation of the form

$$\ln[r_i/(A - r_i)] = B/T + C \qquad (5)$$

was found to fit the r_i data accurately from 77°C to near 1600°C. The B term of eqn. (5) corresponded to a $\Delta H°$ value of 6.4 ± 0.4 Kcal/mole B_3O_6 ring rupture. The A term of eqn. (5) was taken as 0.644, which corresponded to the value of r_i near 77°K.

In the present work it was determined that the assumption relative to $I_{300-800}$ is correct, as shown in Fig. 4. In addition the original r_i data were treated by a computer procedure in which the specific A value corresponding to the minimum standard error of fit for an equation of the form of eqn. (5), was determined. This procedure gave an A value of 0.6449 in good agreement with the previous

value of 0.644. Also, the B and C values were not significantly different from those reported using the A value of 0.644.[4]

As an additional test of the previous $\Delta H°$ value, however, new (absolute) values of I_{800} as well as new relative values of $I_{800}/I_{300-800} = r_i$ were obtained in this work. These values are compared to the previous r_i values in Fig. 5. All of the new I_{800} and r_i data were then treated by eqn. (5) using, for consistency, the original A value of 0.644. The least squares $\Delta H°$ value that resulted is 5.6 ± 1.0 Kcal/mole B_3O_6 ring rupture. However, the difference between this new value and the previous Raman value of 6.4 ± 0.4 Kcal/mole is not very significant as seen from the scatter of the new data of Fig. 5. Further, because the previous $\Delta H°$ value involved more data, and a wider range of temperature, it is still preferred.

D. Accomodation with Neutron Diffraction Results.

Johnson et al.[11] have recently conducted neutron diffraction measurements on vitreous B_2O_3. Their data indicate that 60% of the B atoms exist in the boroxol ring, B_3O_6, configuration at room temperature. However, the results of Ref. (4) would appear to require that the boroxol ring concentration is much higher at room temperature and thus it is desirable to attempt a reconciliation between the two sets of results.

In the work of Ref. (4) all of the r_i data from 77°K to 1600°C were treated as though the equilibrium existing at higher temperatures between boroxol rings, and BO_3 triangles in a random network, continued to manifest itself below T_G. But, it is virtually certain that the equilibrium concentrations that exist just above T_G, are "frozen-in" below T_G. Hence, although the previous treatment fitted all of the data from ~77°K to 1600°C empirically, it totally disregarded the nonequillibrium situation below T_G. To correct this, only the data from Ref. (4) above 480° and extending to 1594°C were used, and the A value of 0.6449 was corrected using the neutron data. The corrected A value is given by $A = 0.6449[0.6 + (0.4/3)]/0.6 = 0.7882$, where it was assumed that three BO_3 triangles share three oxygen atoms to form one B_3O_6 unit. Then an equation

CAPTION

Fig. 5. Values of r_i taken from Ref. (4), dashed line, compared with values of I_{800} and $r_i = I_{800}/I_{300-800}$ from the present work, various points.

⊙ - r_i - back-scattering

● - I_{800} - back-scattering

△ - r_i - 90-degree scattering, normalized to r_i from Ref. (4).

⊡ - I_{800} - 90-degree scattering, normalized to r_i from Ref. (4).

Fig. 5

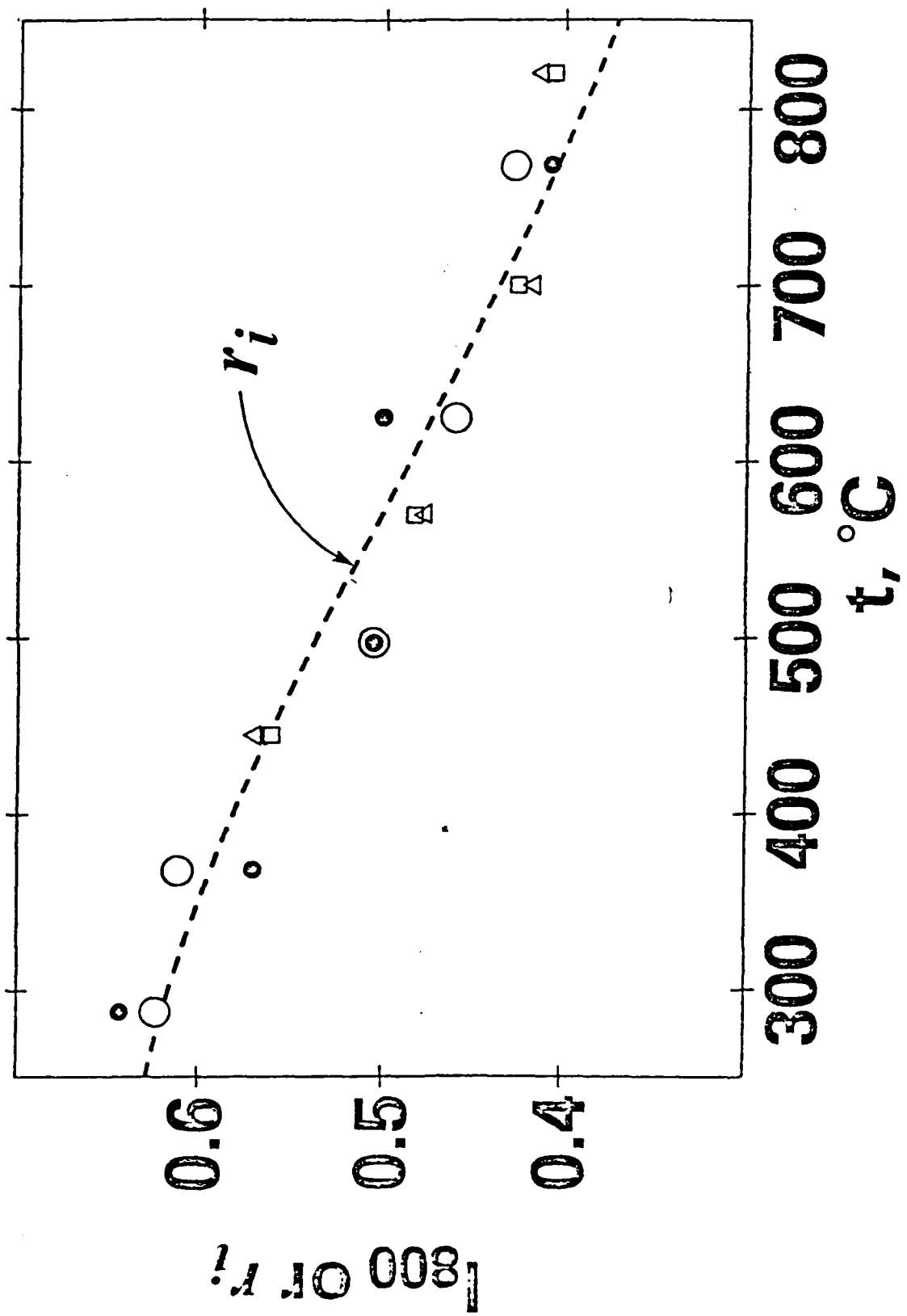

equivalent to eqn. (5) was fit by exponential least squares which yielded a $\Delta H°$ value of 5.0 Kcal/mole boroxol.

Leidecker et al.[12] have applied a formalism involving a single ground state and a twofold degenerate excited state to specific volume and other data from vitreous and molten B_2O_3. They obtained a ΔH value of 5.07 (±2%) Kcal/mole. The value from Ref. (4) is seen to be about 1.3 kcal/mole higher than the Leidecker value, whereas the neutron corrected value of 5.0Kcal/mole is in excellent agreement. The new calculation method which employs the neutron data also has the advantage that it treats the region near and below T_G explicitly, and it also specifically considers the neutron determined fraction of BO_3 triangles in the random network configuration. The agreement between the neutron corrected Raman $\Delta H°$ value and the Leidecker result also indicates that the Leidecker value refers to the heat per mole of boroxol ring. Finally, the differences between the measured r_i values and those calculated from $\ln[r_i/(0.7882 - r_i)] = 2490.5/T - 2.3734$ (the neutron corrected least squares equation) constitute a possible measure of the metastability of the vitreous material relative to the supercooled melt (no glass transition).

E. Relation Between the Low-Frequency Raman Data and T_G

In Fig. 3 peak frequency values from the $I_R/(1+n)$ spectra (upper curve) and from the uncorrected I_R spectra (lower curve) are plotted from -265°C to 1000°C. The T_G value for B_2O_3 of 280°C taken from Marcedo et al.[11] is shown on the figure.

The peak frequencies from the B.-E. corrected spectra, $I_R/(1 + n)$ are seen to be roughly constant, $\sim$50 cm^{-1}, from -265°C to about 100-200°C, but just below T_G, they start to decrease. A rapid decrease then occurs above T_G, and a levelling off to about 27 cm^{-1} occurs above 400-500°C, continuing to 900°C.

The uncorrected spectra yield a somewhat more complicated shape. Near -265°C or 8°K, the peak frequency occurs near 50 cm^{-1} in agreement with the B.-E. corrected result. This agreement arises, of course, because $(1 + n) \rightarrow 1$ as $T \rightarrow 0$. Then between -265°C and -200°C an abrupt decrease of the peak frequency occurs and from -200 to

about 200°C the peak frequency is about constant at 27 cm^{-1}. Next, a decrease is seen just below T_G and a roughly constant value near $\sim$8 cm^{-1} is finally attained between 500° to 1000°C.

After the abrupt initial decrease in the peak frequency from $\sim$50 to $\sim$27 cm^{-1} is complete at $\sim$73°K, where $KT \approx 51$ cm^{-1}, the difference between the corrected and uncorrected peak positions remains roughly constant. At -200°C (or 73°K) the difference is $\sim$22 cm^{-1}, and at 1000°C it is $\sim$20 cm^{-1}. This roughly constant difference is not B.-E. related, but arises because one of the two curves of Fig. 3 more accurately represents the true density of states. In this regard, because no known volume effect follows the uncorrected peak frequency change below 73°C, it would appear that the $I_R/(1 + n)$ spectra, which correspond to $c(\omega)\alpha\omega$, more accurately represent the true density of states, as shown next.

Macedo et al.[13] have observed that the specific volume of vitreous B_2O_3 rises markedly above T_G = 280°C, but that the rate of increase decreases continuously to 1400°C. Both curves of Fig. 3 show a very pronounced decrease in peak frequency just above T_G = 280°C. This observation, in conjunction with the specific volume data, suggests that the peak vibrational frequency is modulated by the specific volume. Or, as an approximation, the inverse of either curve of Fig. 3 from 0° to 1000°C roughly parallels the specific volume data.(However, much better correlation with $1/\beta$ is discussed in section IVF).

From previous Raman work,[4] it was shown that the breakdown of boroxol rings begins essentially at T_G and continues to $\sim$1600°C. The network structure of B_2O_3 would thus be expected to change markedly above T_G, namely, from one with many boroxol rings, to one more nearly dominated by a network of BO_3 triangles. In such a transformation the volume of voids, or the free volume,[14] would be expected to increase, giving rise to the observed increase in the specific volume.

The increase in the free volume should have marked effects on the force constant of a large collective mode of the type envisioned here. The potential for such a mode is certainly anharmonic, despite the harmonic approximation used in IVA. Further, the side of the anharmonic potential due to large amplitude motions, would be expec-

ted to show less curvature near the equilibrium position when the free volume is small, then when the free volume is large due to boroxol ring breakdown. An increase in free volume would be expected to decrease the repulsion that a large amplitude motion would otherwise experience when boroxol rings are present. Because the force constant is equal to the curvature of the potential at the equilibrium position, $(\partial^2 v/\partial r^2)$ at r_e, a decrease in the force constant, K, would be expected with an increase in anharmonicity.

In regard to an increase of the force constant with decrease of free volume, it should also be mentioned that the B.-E. corrected peak position (but not the uncorrected one) of the low-frequency contour moves upward with pressure rise (8 kbar), and thus with decrease of specific volume, at room temperature.[15] This result strongly supports an increase of K with decreasing volume. It also supports the B.-E. corrected spectra, $I_R/(1 + n)$, as possibly the best representation for the low-frequency density of states, as further seen from a summary of the present data in Table III.

Caption

Table III. Tests of the success of various representations of the low-frequency vibrational density of states signified by (YES), according to indicated conditions.

Table III

Representation	Constancy of Peak or component Frequency < 73°K	Constancy of integral from 0-300 cm^{-1}	Pronounced Inflection Above T_G	Increase of Peak Frequency under Pressure
I/T or I	NO (I)	YES (I/T) (4%)	YES (I)	NO
I/(1 + n)	YES	YES (6%)	YES	YES
$I\,\Delta\bar{\nu}/(1+n)$	YES	YES (8%)	NO	uncertain because of large breadth

TABLE III

F. Relation to Ultrasonic Stress Waves in Isotropic Media and Brillouin Scattering.

An overview of all of the Raman data of this work strongly suggests an interpretation involving ultrasonic (GHz to THz frequencies) stress or acoustic waves in an isotropic viscoelastic medium. In this regard, it has been known for many years that materials exist whose response to stress is strongly time (frequency) dependent, for example, rubber. Young's modulus, E, is very strongly decreased at low frequencies, 10^{-2} to 10^{6} Hz, by the melting of rubber. But, if frequencies of 10^{8} Hz are involved, the value of E corresponding to the frozen condition is retained at temperatures well above the freezing point. By comparing Fig. 3 of this work, to Fig. 1 from the work of Nolle[16] for rubber, it is apparent that analogous situations may exist, particularly if it is also noted that the frequency of the nominal 800 cm^{-1} optical mode due to boroxol rings is constant to within 1-2 % from 8°K to 1500°K. Thus, such comparisons suggest that the frequency responses seen in the Raman data may be a measure of the time dependent response of the strain, to thermally-driven stresses.

From the theory of wave propagation in isotropic elastic media, it is known that the velocity of the longitudinal dilatational wave, c_1, is explicitly related to the bulk modulus, $\mathcal{K}$, and hence to the compressibility, $\beta = \frac{-1}{V}\left(\frac{\partial V}{\partial P}\right)_T$, where $\mathcal{K} = 1/\beta$. For a scalar disturbance the longitudinal velocity is given by $\rho\, c_1^{\,2} = \mathcal{K} + 4\mu/3$, and for a shearing disturbance, the velocity of the transverse wave, c_2, is given by $\rho c_2^{\,2} = \mu$, where μ, and ρ, are the shear modulus, and the mass density, respectively.

Values of β have been reported for B_2O_3 from $\sim 280°$ to 800°C.[17] From these data, a marked decrease in $\mathcal{K}$ is expect- from $\sim$ 280-516° C, followed by near constancy to 800°C. Frequency variations remarkably similar to the variations in $\mathcal{K}$ are evident in the Raman data between 280-800°C. From Fig. 3 the B.-E. corrected peak position is seen to decrease markedly from T_G to about 500°C, and then to remain nearly constant to 900°C. Moreover, the B.-E. corrected Raman frequency increases with pressure rise to 8 kbar for the vitreous solid at room temperature, and because $\mathcal{K} = \varrho(\partial p/\partial \varrho)_T \approx$ const x ϱ, $\mathcal{K}$ would be expected to increase with pressure rise. Thus, the dependence of the low-frequency peak position on $\mathcal{K}$ is in accord with stress wave theory. A test of the $\mathcal{K}$ or $1/\beta$ dependence of the B.-E. corrected low-frequency peak position is shown in Fig. 6. The obvious linearity between $\Delta\bar{\nu}$ and $\mathcal{K}$ between 200° and 800°C illustrates the point that the bulk modulus modulation of $\Delta\bar{\nu}$ is much more direct than the $1/\bar{V}$ or ϱ modulation mentioned previously in section IV. E.

A further feature of the present Raman data is the virtually complete depolarization observed for the low-frequency Raman contour. In terms of a cluster of the type described in section IV. A., it may be seen that translation of the cluster compresses the B-O-B angles of one end, while the same translation opens the B-O-B angles at the other end. This coupled 180° phase difference alone is sufficient to lead to depolarization,[18] because it is the B-O-B bending vibration that produces the Raman activity, whereas no polarization or polarizability change is considered to occur within the cluster, as far as the low-frequency region is concerned. However, the depolarization mechanism described may be incorporated into the stress wave theory through the symmetries of the particle

CAPTION

Fig. 6. Plot of B.-E. corrected low-frequency Raman peak position versus bulk modulus, $\mathcal{K} = 1/\beta$, for vitreous and molten B_2O_3 from 200° to 800°C, see temperatures next to points. Data were obtained by interpolation from smoothed curves of Fig. 3, and Ref. (17).

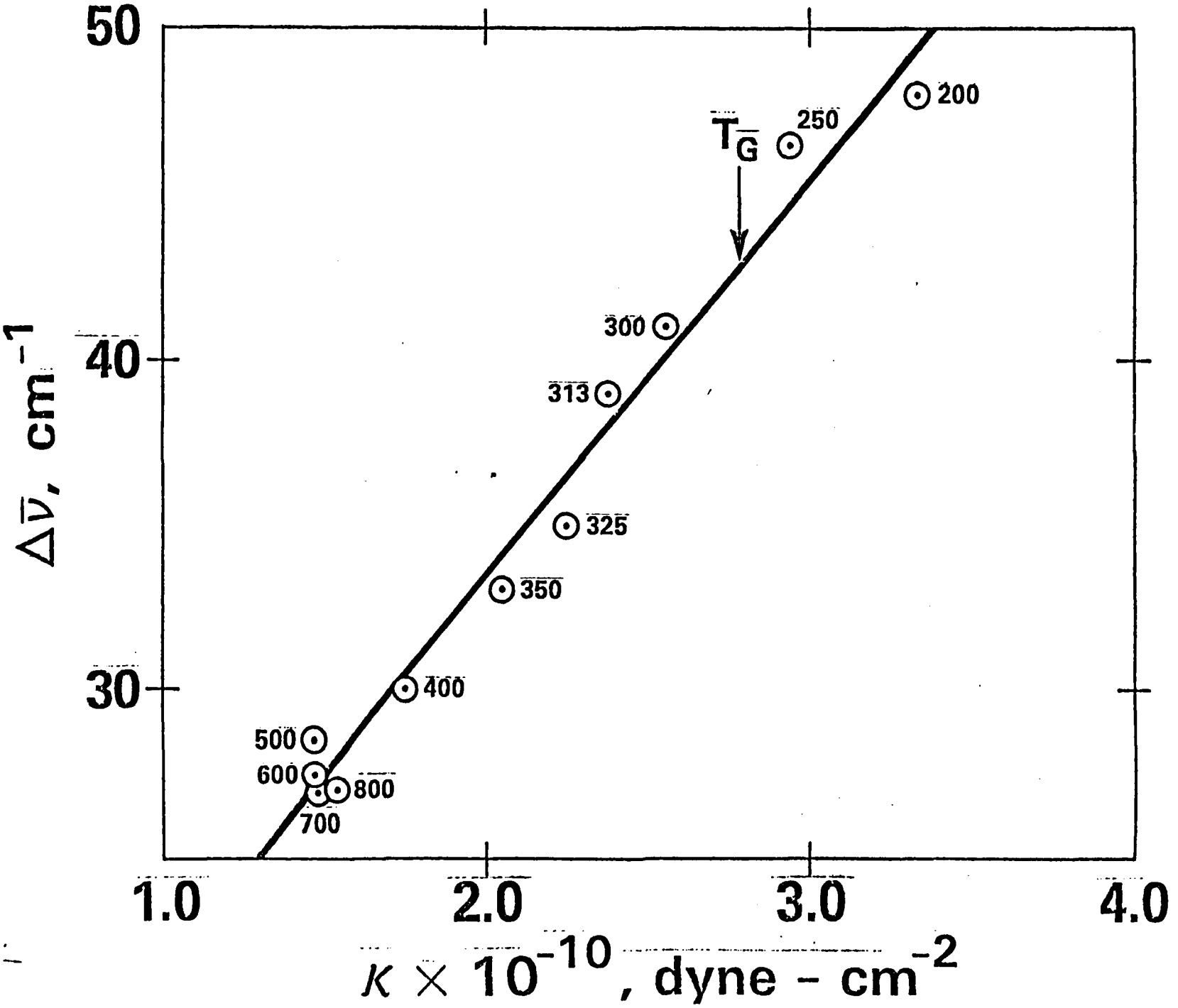
50
40
30
1.0
2.0
3.0
4.0
$\Delta\bar{\nu}$, cm^{-1}
$K \times 10^{-10}$, dyne - cm^{-2}
T_G
200
250
300
313
325
350
400
500
600
700
800

Fig. 6

motions.

Consider that the low-frequency Raman or acoustic modes of vitreous and molten B_2O_3 can be treated in terms of the normal modes of vibration of an isotropic elastic sphere.[19] Such modes may be divided into three classes, namely, radial, spheroidal, and toroidal (rotatory), or R, S, and T, respectively.[20] The R and S modes are longitudinal modes that involve dilatation. They propagate with the velocity, $c_1 = \sqrt{(\kappa + 4\mu)/\rho}$. The T modes are transverse modes related to shear, and they propagate with a velocity $c_2 = \sqrt{\mu/\rho}$. The R modes are of particular interest here.

The lowest order R mode of a sphere is a totally symmetric breathing mode, and would thus refer to <u>polarized</u> Raman scattering. However, because it also refers to a small M' ratio, it is not a collective mode of the type described previously. The next higher mode, however, is of direct interest. This mode is related to a double couple, and refers to vibrations of a sphere in four quadrants. The modal pattern of the radial particle displacements is described by the function $\sin 2\theta \cos\phi \hat{r}$.[19] This pattern can be described by two orthogonal pairs of lobes (like d orbitals). The particle motions of one pair of lobes are inward toward the origin, whereas the particle motions of the other pair are outward. Such particle motions correspond to the B_{2g} motion of the D_{4h} point group, and would thus lead to <u>depolarization</u> of the corresponding <u>longitudinal acoustic</u> Raman scattering. Here, one temporal cluster is envisioned to occupy <u>each</u> or the four lobes, with the nodal regions relating to the one-phonon B-O-B bending regions that restrain and separate the moving clusters. It is also important to note that this depolarized mode refers to the

quantity $\mathcal{K} + 4\mu/3$, i.e., its frequency would be modulated by the bulk modulus, in agreement with Fig. 6. The double couple also involves transverse acoustic modes for which the particle motions are perpendicular to the axes of the radial lobes. These motions refer to the function $\cos 2\theta \cos\phi \hat{\theta} - \cos\theta \sin\phi \hat{\phi}$, and they differ in phase by 180° between successive quadrants. This coupled phase difference relates the shear modes to the Raman depolarization. The modulus involved in this case is μ.

Another feature related to stress waves in viscoelastic, as opposed to elastic, isotropic media is important in describing the nature of the temporal clusters envisioned here. A correlation length of 10 - 15 A was suggested previously. This length refers to a situation in which the movements of the elements of the temporal cluster lose phase coherence beyond 10 - 15 A. In acoustic terms, such a cluster may refer to a disturbance that is strongly damped in a distance L = 10 - 15 A, where L is the distance in which the acoustic intensity, I, falls to I_o/e, i.e., $L = 1/\alpha$, where α is the acoustic absorption coefficient. For real solids, α is a strongly ($\sim\omega^2$) increasing function of frequency. Thus, high-frequency acoustic waves would lead to a small L value, say 10 - 15 A. Such high-frequency sound waves would act as a grating for the scattering of photons or neutrons, and thus the stress wave interpretation of the Raman data can in principle be related to Brillouin scattering, or perhaps more directly to neutron scattering, which involves a larger momentum transfer, and refers to frequencies in the THz region.

Brillouin scattering measurements have been reported for vitreous and molten B_2O_3 by Bucaro and Dardy,[17] by Pelous,[21] and by Day and Bucaro.[22] The measurements of Bucaro and Dardy involved polarized and depolarized scattering at temperatures from 20°C to 516°C. From depolarized scattering a quantity, S_{HV}, was obtained, which is the spatial correlation function of the anisotropic induced polarization.[17] The quantity S_{HV} indicated a variation between 20-516°C very close to that observed for r_1 in Ref. 4, and hence S_{HV} probably relates primarily to boroxol rings, whose concentrations would be "frozen-in" below T_G, as suggested in section IV.E., and also by Bucaro and Dardy. Pelous obtained values of the Brillouin shift ($\sim$ proportional to c_1) and the linewidth ($\sim$ proportional to the absorption coefficient, α) at frequencies of $\sim$ 20GHz from 3-300°K. Day and Bucaro also obtained Brillouin shifts and frequencies, but in the $\sim$ 10-14 GHz region from 20°C to 628°C. Day and Bucaro's linewidth data indicate a strong maximum near 500°C, and this result is probably consistent with the linewidth data of Pelous, which begin to rise sharply at about 30°C.

Jäckle[23] has shown that the acoustic absorption coefficient, α, is expected to be proportional to $g(\omega)$ and hence to $\omega\, I(\omega,T)/\left[1 + n(\omega,T)\right]$, if the stress waves and the Raman scattering are related. In view of this relationship, it is not clear how the maximum in α observed by Day and Bucaro near 500°C relates to the present Raman observations, namely, that the B.-E. corrected contour amplitude just above 7.5 cm^{-1} (as well as the total contour

intensity) are independent of temperature above T_G. The difficulty probably involves comparisons between widely disparate frequencies, that is, 10-14 GHz compared to 200 GHz or above, i.e., the very large aggregates that might be associated with 10-14 GHz (1/3 to 1/2 cm^{-1}) might not be expected to survive at the higher temperatures.

Finally, the general features of the B.-E. corrected Raman spectra (here preferred as a representation of the density of states) are similar from T_G to 900°C, cf., Fig. 2(a). Hence, if large aggregates are considered to experience about the same mean restoring field, the B.-E. corrected spectra may be considered to represent, at least qualitatively, the size or mass distribution of the melt. Thus, from Fig. 2(a), it is apparent that the contribution of masses larger than those associated with the peak intensity falls rapidly ($\Delta\bar{\nu} < 27$ cm^{-1}), compared to the distribution of the lighter masses ($\Delta\bar{\nu} > 27$ cm^{-1}). Apparently, the mass or size distribution begins with (librations or translations of) BO_3 triangles (~ 170 cm^{-1}), and extends to aggregates in excess of the peak value of $\sim$ 23,000 g/mole. In the vitreous solid, of course, the mean restoring force or modulus increases relative to the melt. However, a similar size or mass distribution still exists, because the distribution existing at T_G would be "frozen-in" at lower temperatures.

SUMMARY

Low-frequency Raman spectra have been obtained from vitreous and molten B_2O_3 from 8°K to 900°C. The low-frequency contour intensities fit the one-phonon B.-E. relation closely above T_G, and the B.-E. corrected peak frequency decreases above T_G in a manner suggestive of viscoelastic behavior. The low-frequency Raman contour from 0 - 300 cm^{-1} appears to represent a distribution of masses or sizes involving BO_3 triangles, B_3O_6 rings, and increasingly larger aggregates involving, for example, 400 BO_3 units. The temperature dependence of the B.-E. corrected peak frequency was found to be linear in the bulk modulus, strongly suggesting a connection with stress wave theory. The virtually complete depolarization of the low-frequency Raman contour may also be explained by the symmetry properties of longitudinal and transverse acoustic modes whose frequencies lie in the GHz to THz region.

Acknowledgements

The authors wish to thank the Office of Naval Research for two contracts which made this work possible.

REFERENCES

1. R. H. Stolen, Phys. and Chem. Glasses 11, 83(1970).
2. R. Shuker and R. W. Gammon, J. Chem. Phys. 55, 4784(1971).
3. T. W. Bril, Doctoral Dissertation, Eindhoven, 1976.
4. G. E. Walrafen, S. R. Samanta, and P. N. Krishnan, J. Chem. Phys. 72, 113(1980).
5. R. H. Stolen and G. E. Walrafen, J. Chem. Phys. 64, 2623(1976).
6. M. L. Prod'homme, J. Phys. Radium 18, 75(1957); J. H. Wray and J. T. Neu, J. Opt. Soc. Am. 59, 774(1969).
7. S. Guha and G. E. Walrafen, Phys. Rev. submitted 1983.
8. J. A. Bucaro and T. A. Litovitz, J. Chem. Phys. 54,3846(1971).
9. R. Shuker and R. W. Gammon, Phys. Rev. Lett. 25, 222(1970).
10. The intensity of scattering from a polarized Raman line decreases to zero as the angle of scattering goes to zero.
11. P. A. V. Johnson, A. C. Wright, and R. N. Sinclair, AERE-R10173, Harwell, Oxfordshire, England, August 1981.
12. H. W. Leidecker, J. H. Simmons, T. A. Litovitz, and P. B. Macedo, J. Chem. Phys. 55, 2028(1971).
13. P. B. Macedo, W. Capps, and T. A. Litovitz, J. Chem. Phys. 44, 3357(1966).
14. M. H. Cohen and G. S. Grest, Phys. Rev. B, 20, 1077(1979).
15. S. Guha and G. E. Walrafen, Phys. Rev. submitted 1983.
16. A. W. Nolle, J. Polymer Sci. 5, 1(1948).
17. J. A. Bucaro and H. D. Dardy, J. Appl. Phys. 45, 5324(1974)
18. This statement is true only for certain point groups, e.g., C_2, etc.

19. K. Aki and P. G. Richards, "Quantitative Seismology, Theory and Methods, Volume I", W. H. Freeman and Co., San Francisco, 1980.

20. $R_\ell^m(\Delta,\phi) = Y_\ell^m \hat{r}$; $S_\ell^m(\Delta,\phi) = \frac{1}{[\ell(\ell+1)]^{1/2}}\left(\frac{\partial Y_\ell^m}{\partial \Delta}\hat{\Delta} + \frac{1}{\sin\Delta}\frac{\partial Y_\ell^m}{\partial \phi}\hat{\phi}\right)$;

$T_\ell^m(\Delta,\phi) = \frac{1}{[\ell(\ell+)]^{1/2}}\left(\frac{1}{\sin\Delta}\frac{\partial Y_\ell^m}{\partial \phi}\hat{\Delta} - \frac{\partial Y_\ell^m}{\partial \Delta}\hat{\Phi}\right)$, see Ref. (19).

21. J. Pelous, Physics Lett. 74A, 275(1979).

22. D. K. Day and J. A. Bucaro, private communication and doctoral dissertation of the former, Naval Research Laboratory, Washington, D. C.

23. J. Jäckle in "Amorphous Solids, Low-temperature Properties", W. A. Phillips, ed., Springer-Verlag, Berlin. (Volume 24 of the Topics in Current Physics series).


DAT
FILM